Supporting Information for "The Greater Mekong's climate-water-energy nexus: how ENSO-triggered regional droughts affect power supply and CO_2 emissions"

AFM Kamal Chowdhury[1,2], Thanh Duc Dang[1], Hung Tan Thai Nguyen[1],

Rachel Koh[1], Stefano Galelli[1]

[1]Pillar of Engineering Systems and Design, Singapore University of Technology and Design, Singapore 487372

[2]Environmental Studies Department, University of California Santa Barbara, Santa Barbara CA 93106-3060

Contents of this file

1. Section S1 to S3:

   (i) Section S1: Setup and Validation of PowNet

   (ii) Section S2: Setup, Calibration, and Validation of VIC-Res

   (iii) Section S3: Water availability simulation outside the Mekong and Chao Phraya River basins

2. Tables S1 to S4 with captions:

   (i) Table S1: Design specifications of the hydropower dams

   (ii) Table S2: Freshwater-dependent capacity of the thermoelectric plants

   (iii) Table S3: Economic and technical parameters of the power plants

   (iv) Table S4: Classification of the years as El Niño, Neutral, and La Niña

————

September 21, 2020, 2:58pm

3. Figures S1 to S7 with captions:

(i) Figure S1: VIC-Res performance in calibration and validation

(ii) Figure S2: Simulated vs expected hydropower production

(iii) Figure S3: Comparison between VIC-Res and FLO1K

(iv) Figure S4: Exposure of hydropower and freshwater-dependant thermoelectric plants to hydro-climatic variability

(v) Figure S5: Annual derated capacity for gas, coal, biomass and waste heat plants

(vi) Figure S6: Composite analysis

(vii) Figure S7: Hourly spinning and non-spinning reserves

S1. Setup and Validation of PowNet

To setup PowNet, we used the values of the technical and economic parameters reported in Table S3. We then proceeded to validate the model by comparing the simulated and observed values of generation mix and production costs for the year 2016. The 198,100 GWh produced by the Laotian–Thai power system were generated by the following mix: 63.2% natural gas, 18.6% coal, 9.9% import from Laos (coal and hydro), 6.2% biomass, 1.8% domestic hydro, and less than 1% oil, wind, and solar (EGAT, 2016; IRENA, 2017). All these figures are simulated by PowNet with an error lower than 5%. As for the production costs, our estimate is 9.7 billion USD, slightly lower than the 12.5 billion USD ($\sim$ 395.5 billion Baht) reported by EGAT (2016). This underestimation may be due to various factors—such as the operating costs of domestic hydro, solar, and wind power plants, which are not accounted for by PowNet. To estimate the CO_2 emissions, we post-processed the simulated data on the generation mix and applied the following rates: 1.04 (coal), 0.47 (gas), and 0.73 (oil) tonnes of CO_2 per MWh (Mittal et al., 2014). The 99.2 Mtonnes emitted in 2016 (EPPO, 2017) are simulated with an accuracy of 95%.

S2. Setup, Calibration, and Validation of VIC-Res

S2.1. Setup

To setup VIC-Res, we used the same input data for both Mekong and Chao Phraya River basins. As mentioned in Section 2.3, rainfall and temperature data were taken from APHRODITE (Asian Precipitation – Highly-Resolved Observational Data Integration Towards Evaluation, Yatagai et al. (2012)) and CFSR (Climate Forecast System Reanalysis, Saha et al. (2014)), respectively. Land use and cover data were ob-

tained from the Global Land Cover Characterization dataset, developed by the United States Geological Survey (`https://www.usgs.gov/centers/eros/science/`), while the soil data were extracted from the Harmonized World Soil Database, developed by the International Institute for Applied System Analysis and the Food and Agriculture Organization (`http://www.fao.org/soils-portal/soil-survey/soil-maps-and-databases/harmonizedworld-soil-database-v12/en/`). Both datasets have a spatial resolution of 30 arcsecond (while our VIC-Res implementation has a resolution of 0.0625 degrees), so we proceeded by generating the land use and soil maps with the majority resampling technique, which assigns the most common values found from the group of involved pixels to the new cell. The monthly Leaf Area Index and albedo were derived from the Terra MODIS satellite images, which represent changes in canopy and snow coverage over time. To produce the Digital Elevation Model (DEM) needed for the flow direction map, we proceeded in two steps. First, we masked the Global 30 Arc-Second Elevation DEM with the shape of the two basins, and then adapted it to the resolution of our models with the average resampling technique (Hoang et al., 2019).

To accurately model reservoirs and their operations, VIC-Res needs data on bathymetry, maximum surface extent, dam design specifications, and operating rules. Ideally, one should use the bathymetry produced with either field surveys or by processing remotely-sensed images (Gao, 2015), but this information is not yet available for the large number of reservoirs characterizing our study site. For this reason, we modelled the storage-depth relationship with Liebe's method (Liebe et al., 2005), a common approach in large-scale hydrological modelling studies (Ng et al., 2017; Shin et al., 2019). The maximum sur-

face extent of each reservoir (needed to calculate the evaporation from the reservoir cells) was obtained by extracting surface water profiles from Landsat TM and ETM+ imagery. The dam design specifications, reported in Table S1, were provided by the Mekong River Commission (MRC, 2017) and Electricity Generating Authority of Thailand (EGAT, 2018), and complemented with information extracted from the Global Reservoir and Dam Database and the International Commission On Large Dams' database. Similarly to the bathymetry, the process of inferring the operating rules from satellite images is a very promising field of research (Bonnema & Hossain, 2017), but not yet scalable to the number of reservoirs in our study site. We thus proceeded to adopt the approach proposed by Piman, Cochrane, Arias, Green, and Dat (2013), with which we designed seasonal rule curves that aim to maximize hydropower production—an assumption supported by previous studies (Räsänen et al., 2017). Specifically, the rule curves are designed to draw-down the reservoir storage during the driest months (e.g., December to May) to maximize the electricity production, recharge the depleted storage during the monsoon season, and avoid the risks of spilling water at the end of the monsoon season. Rule curves are tailored to each reservoir within both basins by determining the time at which the minimum and maximum water levels are reached (May and November, respectively), setting the value of the minimum and maximum water levels (the minimum and maximum elevation levels of each reservoir), and finally connecting these points with a piecewise linear function that gives us the daily target level for each calendar day. When designing the rule curves, we compare the mean annual (simulated) hydropower production against the annual design (or expected) production—see Section S2.2—thereby accounting for other factors that affect reservoir operations and, therefore, hydropower production (e.g., flood protection,

downstream water supply). For additional details on the representation of reservoir operations in VIC-Res, please refer to T. D. Dang, Vu, Chowdhury, and Galelli (2020).

S2.2. Calibration and Validation

To calibrate VIC-Res, we used daily discharge data gauged at multiple locations in the Mekong and Chao Phraya basins (provided by the Mekong River Commission and the Thai Royal Irrigation Department; `www.hydro1.net`). Specifically, we focussed on the six main parameters controlling the rainfall-runoff process (T. Dang et al., 2020) and manually tuned them until we attained reasonable values of the Nash-Sutcliffe Efficiency (NSE). The calibration period is 1996–2005; 1995 is used for the model spin-up. Since not all reservoirs in the Mekong were built prior 1995, we only accounted for the reservoirs that were either operational at the beginning of the simulation or that became operational during the horizon considered in the simulation. For the latter, we implemented VIC-Res in such a way to activate the reservoirs at the right time. We did not use filling strategies different from the rule curves described above, because all dams reached a steady-state operation rather quickly. The results illustrated in Figure S1 (left panel) show that the model obtained satisfactory NSE values in both basins.

To validate the models, the first and most immediate step was to compare the simulated discharge for a different observational period, 1985–1994 (with 1984 used for the model spin-up). Also in this case, the timing at which reservoirs became operational was considered explicitly within the simulation. The validation results, reported in Figure S1 (right panel) are inline with the calibration ones. In addition, we compared the mean

annual (simulated) hydropower production against the annual design (or expected) production. For dams in the Mekong, the annual design production is provided by the Mekong River Commission (MRC, 2017); for dams in Thailand, the information is retrieved from EGAT (`https://www.egat.co.th/en/information/statistical-data?view=article&id=78:gross-energy-generation-and-purchase-statistical&catid=15`) and complemented, where necessary, with reports released by dam operators. Results, illustrated in Figure S2, show that VIC-Res attained a reliable level of performance.

S3. Water availability simulation outside the Mekong and Chao Phraya River basins

Within the Laotian–Thai power system, there are seven dams and nine freshwater-dependant thermoelectric stations falling outside the Mekong and Chao Phraya River basins. For these plants, it is still necessary to estimate the water availability, which is in turn necessary to calculate hydropower availability and the adjustment factor of the generation capacity.

For each hydropower reservoir, we estimated the inflow Q_t using the rational method, according to which $Q_t = c \cdot I_t \cdot A$, where c is the runoff coefficient, I_t the rainfall intensity (mm/day), and A the drainage area (km^2). The runoff coefficient was estimated as a function of the soil type and slope of the drainage basins, while the rainfall intensity was extracted from APHRODITE dataset. The inflow was then routed through each reservoir, for which we calculated storage dynamics, release through turbines, hydraulic head, and, finally, available hydropower. The dam design specifications were extracted from EGAT

(2018), while the operating rules were designed by using the same approach described in Section S2.1. To validate the model, we compared the mean annual (simulated) hydropower production with the annual design (or expected) production, shown in Figure S2.

For the thermoelectric stations, we do not need daily water availability data, since the adjustment factor of the generation capacity only depends on the water availability during the driest months. For these sites, we thus used FLO1K, a global streamflow dataset available with a 1-km resolution (Barbarossa et al., 2018). To ensure consistency across the water availability estimated by VIC-Res and FLO1K, we proceeded by comparing the two models across 18 sites in the Mekong and Chao Phraya basins (Figure S3).

References

Barbarossa, V., Huijbregts, M., Beusen, A., Beck, H. E., King, H., & Schipper, A. M. (2018). FLO1K, global maps of mean, maximum and minimum annual streamflow at 1 km resolution from 1960 through 2015. *Scientific Data*, *5*(180052). doi: 10.1038/sdata.2018.52

Bonnema, M., & Hossain, F. (2017). Inferring reservoir operating patterns across the Mekong Basin using only space observations. *Water Resources Research*, *53*(5), 3791–3810.

Dang, T., Chowdhury, A., & Galelli, S. (2020). On the representation of water reservoir storage and operations in large-scale hydrological models: implications on model parameterization and climate change impact assessments. *Hydrology and Earth System Sciences*, *24*, 397–416. doi: 10.5194/hess-24-397-2020

Dang, T. D., Vu, D. T., Chowdhury, A. K., & Galelli, S. (2020). A software package

for the representation and optimization of water reservoir operations in the VIC hydrologic model. *Environmental Modelling & Software*, *126*, 104673. doi: 10.1016/ j.envsoft.2020.104673

EGAT. (2016). *Annual report 2016* (Tech. Rep.). Electricity Generating Authority of Thailand (EGAT).

EGAT. (2018). *Exploring egat dams and thermopower plants* (Tech. Rep.). Electricity Generating Authority of Thailand (EGAT). (url: https://www.egat.co.th/en/images/publication/exploring-EGAT-dams-powerplants-2018.pdf)

EPPO. (2017). *Energy statistics of Thailand 2017* (Tech. Rep.). Ministry of Energy, Thailand: Energy Policy and Planning Office (EPPO).

Gao, H. (2015). Satellite remote sensing of large lakes and reservoirs: From elevation and area to storage. *Wiley Interdisciplinary Reviews: Water*, *2*(2), 147–157.

Hoang, L. P., van Vliet, M. T., Kummu, M., Lauri, H., Koponen, J., Supit, I., . . . Ludwig, F. (2019). The Mekong's future flows under multiple drivers: How climate change, hydropower developments and irrigation expansions drive hydrological changes. *Science of the Total Environment*, *649*, 601–609.

IRENA. (2017). *Renewable energy outlook: Thailand* (Tech. Rep.). Abu Dhabi: International Renewable Energy Agency (IRENA).

Liebe, J., Van De Giesen, N., & Andreini, M. (2005). Estimation of small reservoir storage capacities in a semi-arid environment: A case study in the upper east region of Ghana. *Physics and Chemistry of the Earth, Parts A/B/C*, *30*(6-7), 448–454.

Mittal, M. L., Sharma, C., & Singh, R. (2014). Decadal emission estimates of carbon

dioxide, sulfur dioxide, and nitric oxide emissions from coal burning in electric power generation plants in India. *Environmental Monitoring and Assessment*, *186*(10), 6857–6866.

MRC. (2017). *MRC hydropower database.* (Mekong River Commission (MRC), Vientiane, Lao PDR)

Ng, J. Y., Turner, S. W. D., & Galelli, S. (2017). Influence of El Niño Southern Oscillation on global hydropower production. *Environmental Research Letters*, *12*(3), 10-34. doi: 10.1088/1748-9326/aa5ef8

Piman, T., Cochrane, T. A., Arias, M. E., Green, A., & Dat, N. D. (2013). Assessment of flow changes from hydropower development and operations in Sekong, Sesan, and Srepok Rivers of the Mekong basin. *Journal of Water Resources Planning and Management*, *139*(6), 723-732. doi: 10.1061/(ASCE)WR.1943-5452.0000286

Räsänen, T. A., Someth, P., Lauri, H., Koponen, J., Sarkkula, J., & Kummu, M. (2017). Observed river discharge changes due to hydropower operations in the Upper Mekong Basin. *Journal of hydrology*, *545*, 28–41.

Saha, S., Moorthi, S., Wu, X., Wang, J., Nadiga, S., Tripp, P., ... others (2014). The NCEP climate forecast system version 2. *Journal of Climate*, *27*(6), 2185–2208.

Shin, S., Pokhrel, Y., & Miguez-Macho, G. (2019). High-resolution modeling of reservoir release and storage dynamics at the continental scale. *Water Resources Research*, *55*(1), 787–810.

Yatagai, A., Kamiguchi, K., Arakawa, O., Hamada, A., Yasutomi, N., & Kitoh, A. (2012). APHRODITE: Constructing a long-term daily gridded precipitation dataset for Asia based on a dense network of rain gauges. *Bulletin of the American Meteorological*

Society, *93* (9), 1401–1415.

Table S1. Live storage, design discharge, installed capacity, and year of commission of the hydropower dams operated in the Laotian–Thai water-energy system in the year 2016 (data retrieved from MRC (2017) and EGAT (2018)). Laotian dams are shown in italic.

Basin	Plant	Live storage (Mm^3)	Design discharge (m^3/s)	Installed capacity (MW)	Year of commission
Mekong	*Xeset1*	0.3	33	45	1999
	HouayHo	3.5	23	152	1999
	Xeset2	9.3	33	76	2009
	TheunHinboun	15	106	440	1998
	NamMang3	45	9	40	2005
	NamLeuk	228	40	60	2000
	NamNgum1	1,002	414	155	1971
	NamNgum2	2,425	456	615	2012
	NamTheun2	3,378	334	1075	2010
	LamTakhongJV	297	5.2	500	1974
	PakMun	125	1,105	136	1990
	Chulabhorn	144.5	5	40	1972
	Sirindhorn	1,135	120	36	1971
	Ubolratana	1,854	88	25.2	1966
Chao Phraya	Sirikit	6,668	250	500	1974
	Bhumibol	9,762	694	749	1964
Other	ThungNa	28	231	38	1981
	Kiridharn	56	24.8	12.7	1986
	KaengKrachan	620	37	19.6	1974
	BangLang	1,143	48	72	1981
	Rajjaprabha	4,280	75	276	1987
	Vajiralongkorn	8,100	552	300	1984
	Srinagarind	10,265	140	720	1966

Table S2. Total installed and freshwater-dependent capacity of the thermoelectric plants, organized by fuel type. In the last column, we report the largest, temporary, loss of installed capacity during the period 1976–2005 (see Figure S5 for additional details).

| Type	Total capacity (MW)	Freshwater-dependent capacity (MW)	Seasonal largest derated capacity (MW) over 1976-2005
Coal (Thailand)	5,712	2,765	1,516
Coal import (Laos)	1,878	1,878	751
Gas (Thailand)	24,783	710	454
Biomass (Thailand)	1,555	1,274	524
Waste heat (Thailand)	4,273	1,528	796
Oil (Thailand)	646	-	-

Table S3. Economic and technical parameters of the of the power plants operated in 2016.

The 'slack' generators are used to account for load shedding.

| Type	Heat rate (MMBtu/MWh)	Variable O&M (US$/MWh)	Fixed O&M (U$/MW)	Start-up (U$/MW)	Fuel Price (U$/MMBtu)
Biomass (steam turbine)	14.1	26	1	1	3.02
Laotian coal (steam turbine)	10.05	4.6	2.7	90	5.25
Domestic coal (steam turbine)	10.05	4.6	2.7	90	5
Gas (combined-cycle)	7.65	2	1.2	70	5.85
Gas (gas turbine)	11.21	2	1.7	70	5.85
Gas (internal combustion)	9.18	3.17	1.5	70	5.85
Gas (steam turbine)	11.21	2	1.2	70	5.85
Oil (gas turbine)	13.54	3.17	1.5	50	8
Oil (internal combustion)	10.33	3.17	1.5	50	8
Oil (steam turbine)	10.19	3.17	1.5	50	8
Waste heat (steam turbine)	14.1	26	1.2	50	3.02
Slack (arbitrary generators)	10000	1000	1E+10	1E+10	1000
Laotian hydro-electricity	40 U$/MWh				
Domestic hydro, wind, solar	no operating costs				

Table S4. Years categorized as El Niño, Neutral, and La Niña. We adopt the classification provided by the Japan Meteorological Agency (`https://www.coaps.fsu.edu/jma`) and then shift the years back by one to account for the lag between anomalies of sea surface temperature in the eastern Pacific Ocean and streamflow anomalies in the Mekong and Chao Phraya basin.

ENSO Phase	Year
El Niño	1977, 1983, 1987, 1988, 1992, 1998, 2003
Neutral	1978–1982, 1984–1986, 1990–1991, 1993–1997, 2001–2002, 2004–2005
La Niña	1976, 1989, 1999, 2000
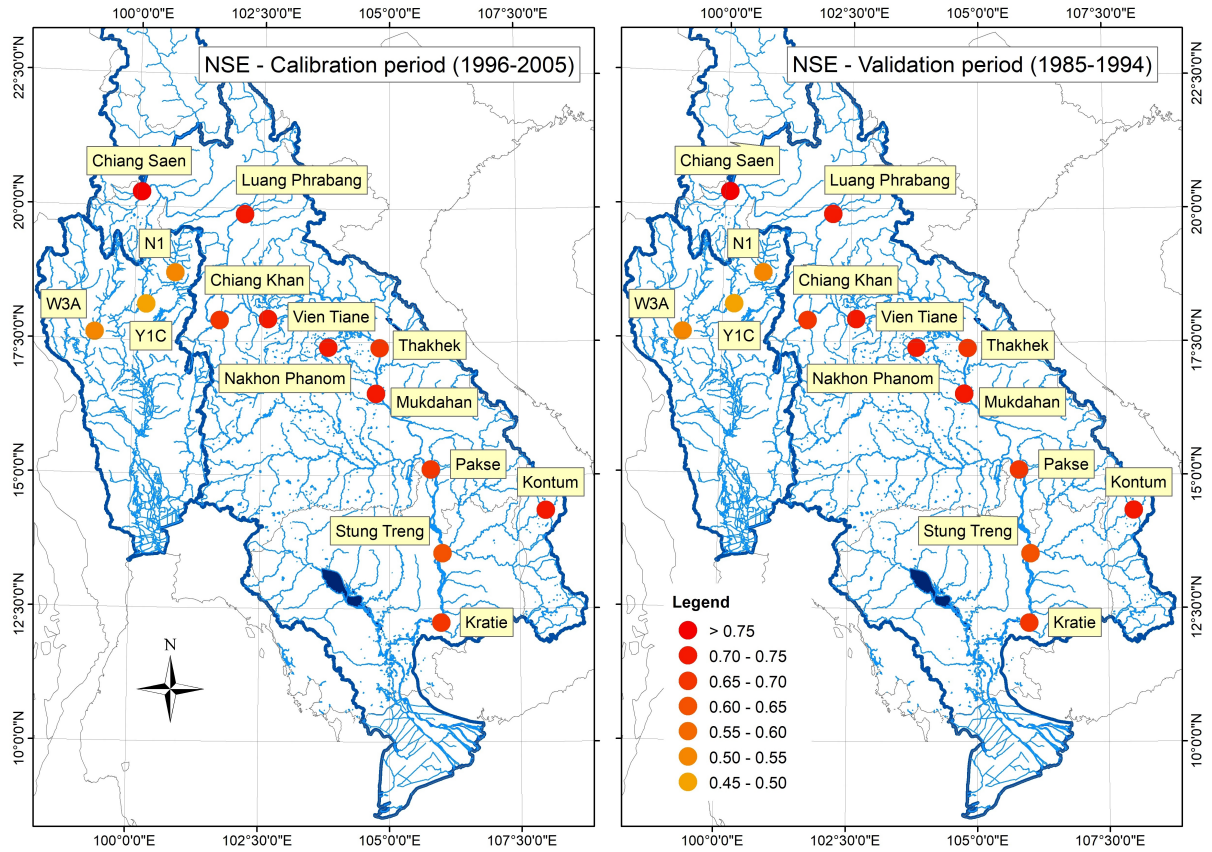
Figure S1. VIC-Res performance on the calibration (1996–2005) and validation (1985–1994) periods in the Mekong and Chao Phraya River basins.
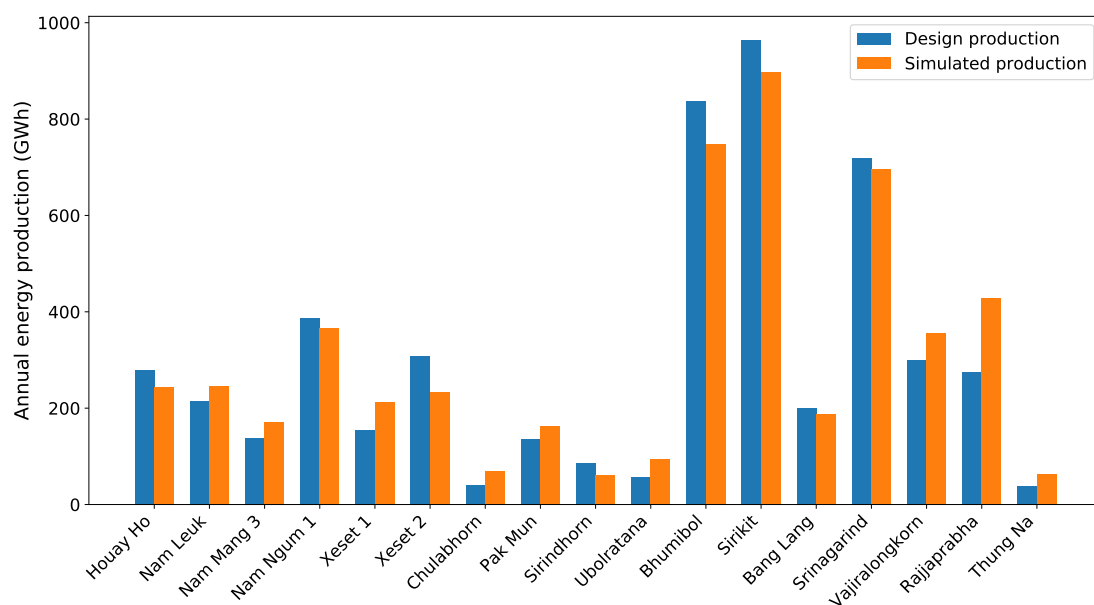
Figure S2. Comparison between the annual design (or expected) production and simulated production (averaged over the period 1976–2005) for 12 reservoirs located in the Mekong and Chao Phraya basins. The analysis includes 5 dams located in smaller basins (BangLang, Srinagarind, Vajiralongkorn, Rajjaprabha, and ThungNa). The reader is referred to Table S1 for the list of reservoirs in the Laotian–Thai water-energy system.
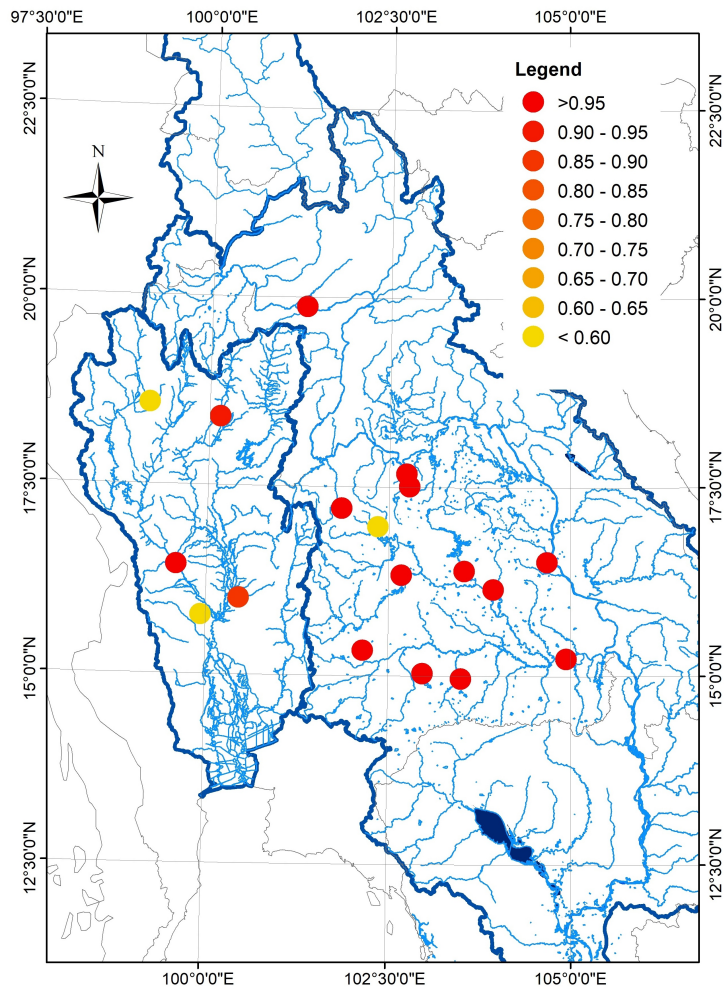
Figure S3. Coefficient of determination (R^2) for the discharge simulated by VIC-Res and FLO1K over the period 1976–2005. The selected sites represent the intake points for the freshwater-dependant thermoelectric stations located in the Mekong and Chao Phraya basins.
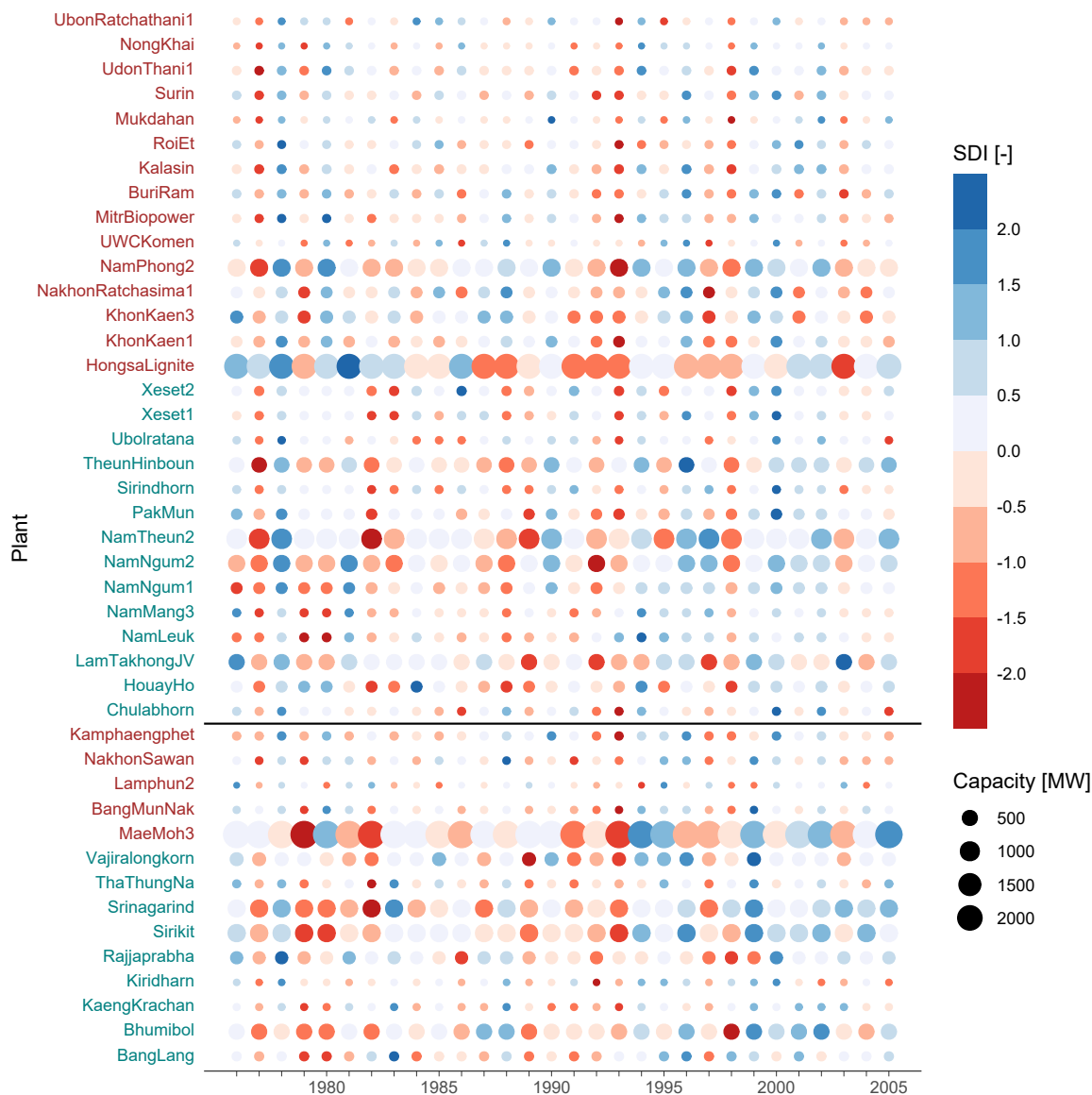
Figure S4. Exposure of hydropower and freshwater-dependant thermoelectric plants to hydroclimatic variability. Plants are listed on the vertical axis, with blue and red representing hydropower and thermoelectric plants, respectively. Plants located in the Chao Phraya basin are listed in the upper part of the plot, while plants in the Mekong basin are reported in the lower part. The exposure of each plant is measured with the SDI, calculated on an annual basis for the area drained by each specific plant. The size of each dot represents the installed capacity.
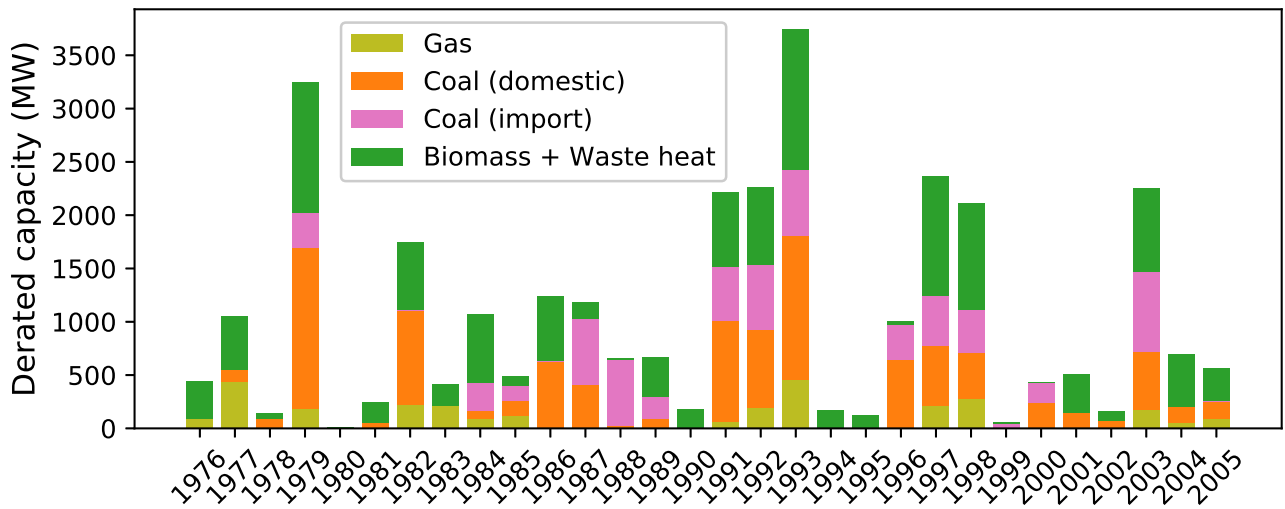
Figure S5. Annual derated capacity for gas, coal (in Thailand and Laos), biomass and waste heat plants. The reader is referred to Table S2 for additional details about the available and derated capacities.
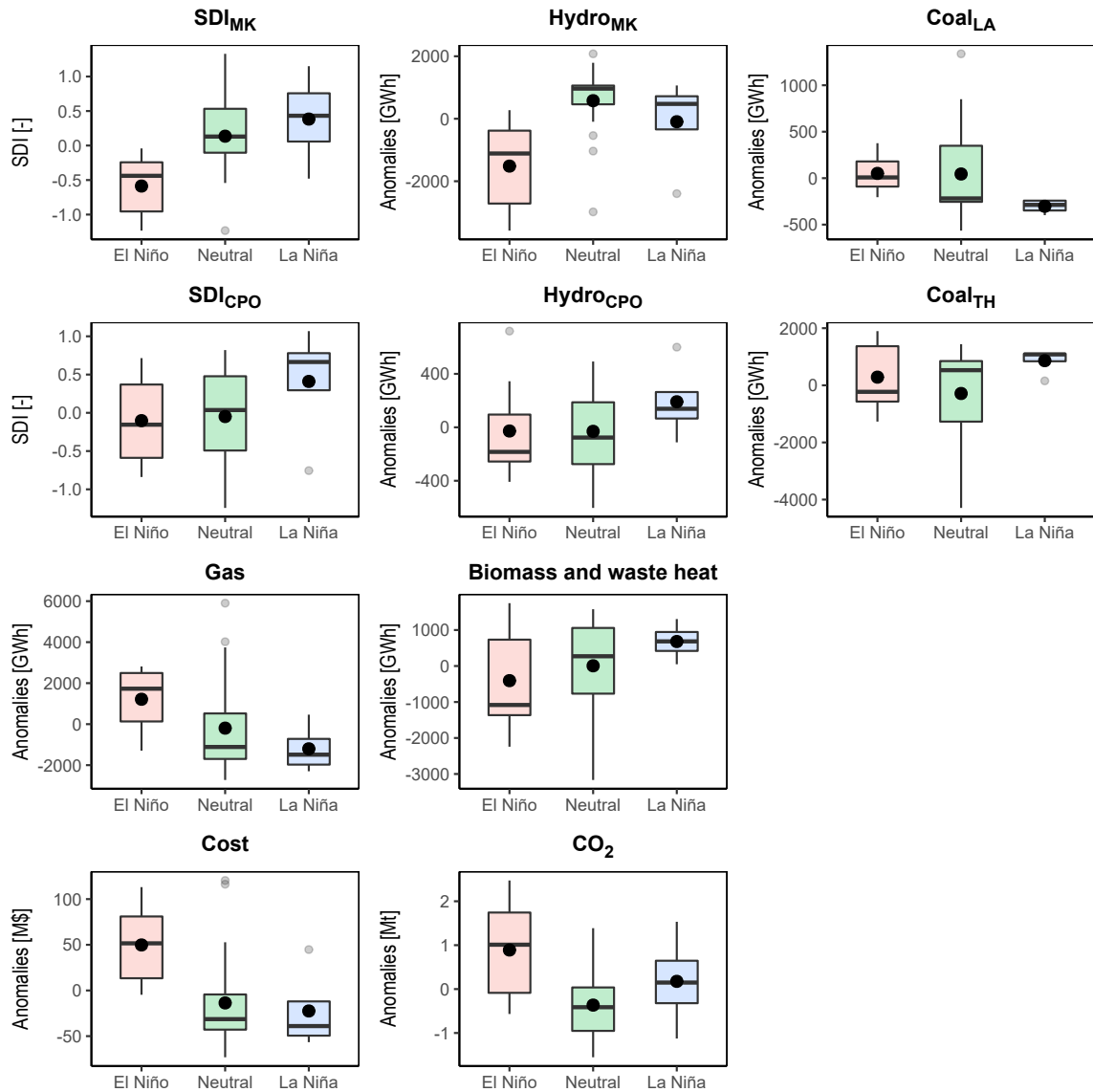
Figure S6. Boxplots illustrating the behaviour of the water-energy system during El Niño, Neutral, and La Niña years. The variables reported here are: state of Mekong and Chao Phraya basins (SDI_{MK} and SDI_{CPO}), production costs, CO_2 emissions, and energy generation mix. For the energy generation mix, we report the electricity dispatched from: hydropower plants located in the Mekong and Chao Phraya ($Hydro_{MK}$ and $Hydro_{CPO}$), coal plants located in Laos and Thailand ($Coal_{LA}$ and $Coal_{TH}$), gas plants (Gas), biomass and waste heat plants (BMWH). In each plot, the median is marked by an horizontal line inside the box, which represents the inter-quartile range. Outliers are outside this range. The large dot within the box represents the mean.

September 21, 2020, 2:58pm
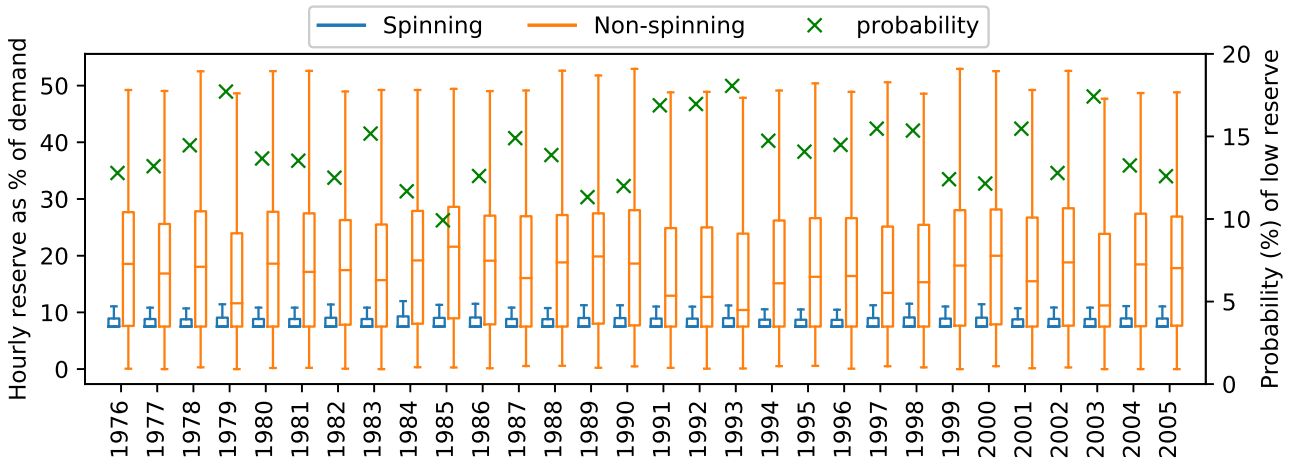
Figure S7. Hourly spinning and non-spinning reserves as a percentage of the instantaneous demand. Results show that the power system mostly maintains the reserves well-above the minimum requirements, i.e., total reserve above 15% of the instantaneous hourly demand, with at least 50% of the reserve as spinning (that is, 7.5% of the total installed capacity). In some instances, the non-spinning reserve reduces to around zero and the minimum requirement of 15% reserve is served as spinning. The green crosses represent the ratio between the amount of such instances in one year over the total number of hours in a year. During dry years (e.g., 1979, 1993, 2003), the probability of low reserve can rise to around 18%.